Cell Stem Cell, Volume *22*

Supplemental Information

YAP/TAZ-Dependent Reprogramming of Colonic Epithelium Links ECM Remodeling to Tissue Regeneration

Shiro Yui, Luca Azzolin, Martti Maimets, Marianne Terndrup Pedersen, Robert P. Fordham, Stine L. Hansen, Hjalte L. Larsen, Jordi Guiu, Mariana R.P. Alves, Carsten F. Rundsten, Jens V. Johansen, Yuan Li, Chris D. Madsen, Tetsuya Nakamura, Mamoru Watanabe, Ole H. Nielsen, Pawel J. Schweiger, Stefano Piccolo, and Kim B. Jensen

Figure S1. Related to Figure 1

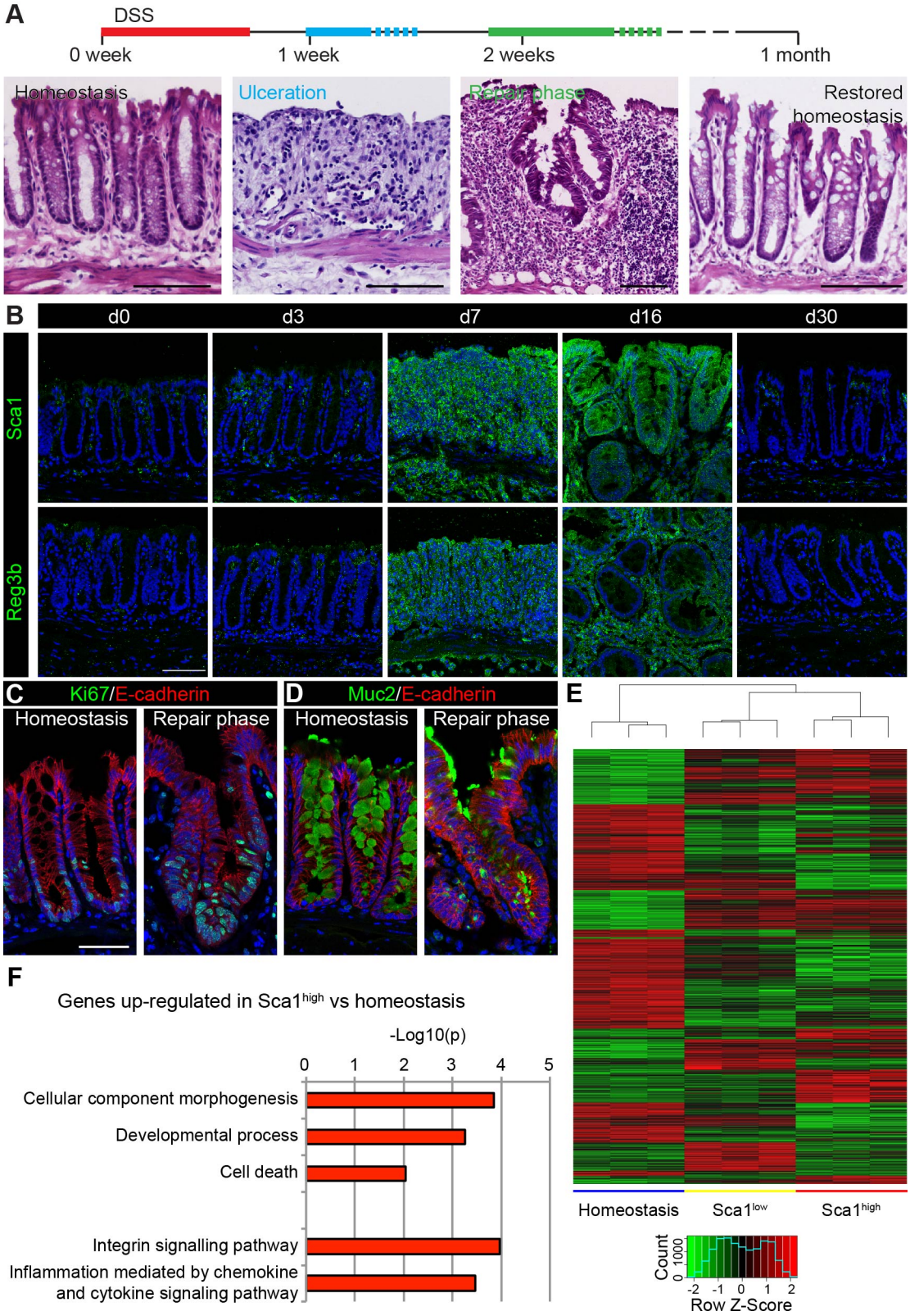

Figure S1: Phases of tissue regeneration following DSS induced colitis

A) Time course of regeneration following DSS induced colitis with representative images of H&E staining of each phase. Scale bars, 100 μm.

B) Time course analysis for expression of Reg3b and Sca1 (both green) during ulceration and regeneration. Tissue is counter stained with DAPI (blue). Scale bar 100μm.

C-D) Ki67 (C) and MUC2 (D) detected during homeostasis and the repair phase. Tissue is counterstained with E-cadherin (red) and DAPI (blue). Scale bar 50μm.

E) Heat map analysis of differentially expressed probe sets (fold change > 2.0, FDR < 0.05) from comparisons of epithelial cells isolated from homeostatic tissue and $Sca1^{low}$ as well as $Sca1^{high}$ cells isolated from mice that have been exposed to DSS.

F) GO term enrichment analysis illustrating biological processes and pathways that are significantly ($p<0.05$) enriched (PANTHER GO slim database) in the $Sca1^{high}$ populations when compared to homeostatic epithelium.

Figure S2. Related to Figure 2

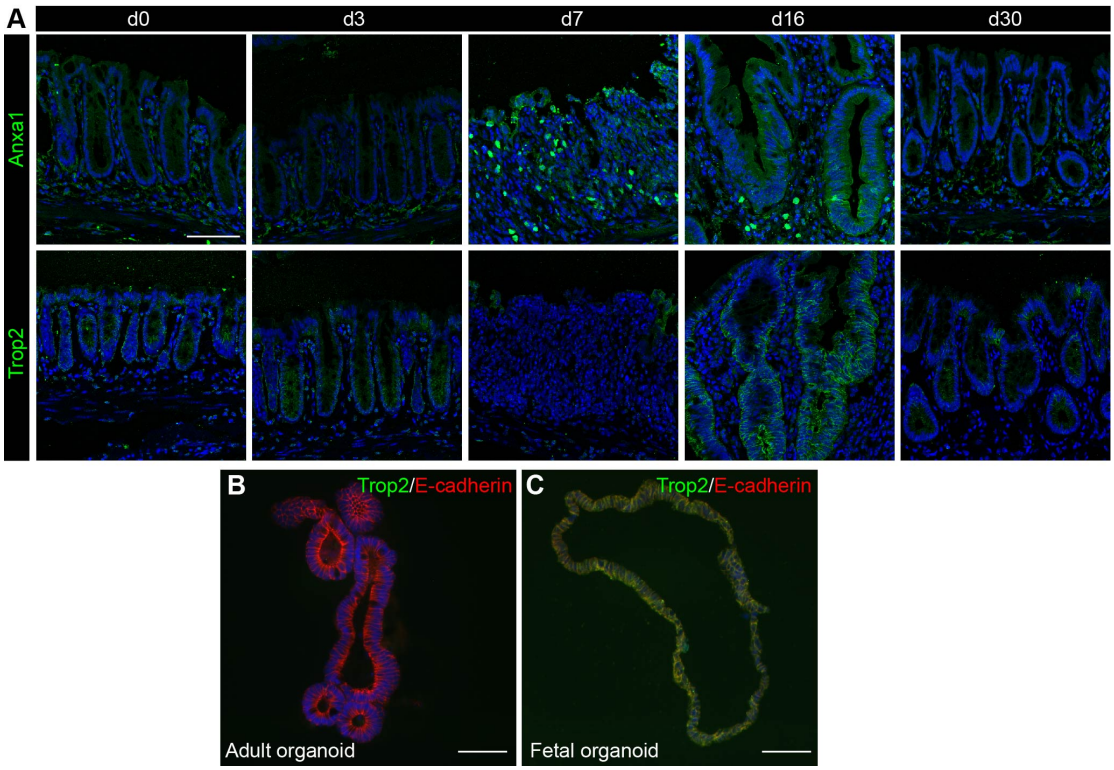

Figure S2: Expression of fetal markers in intestinal epithelium and organoids

A) Time course analysis for expression of the two fetal markers Anxa1 and Tacstd2/Trop2 (both green) during the course of treatment and recovery from experimental colitis. Tissue is counter stained with DAPI (blue). Scale bar 100μm.

B-C) Trop2 (green) expression in organoids derived from the adult small intestine (B) or in enterospheres derived from the fetal small intestine (C). Tissue is counter stained with E-cadherin (red) and DAPI (blue). Scale bar 100μm.

Figure S3. Related to Figure 3

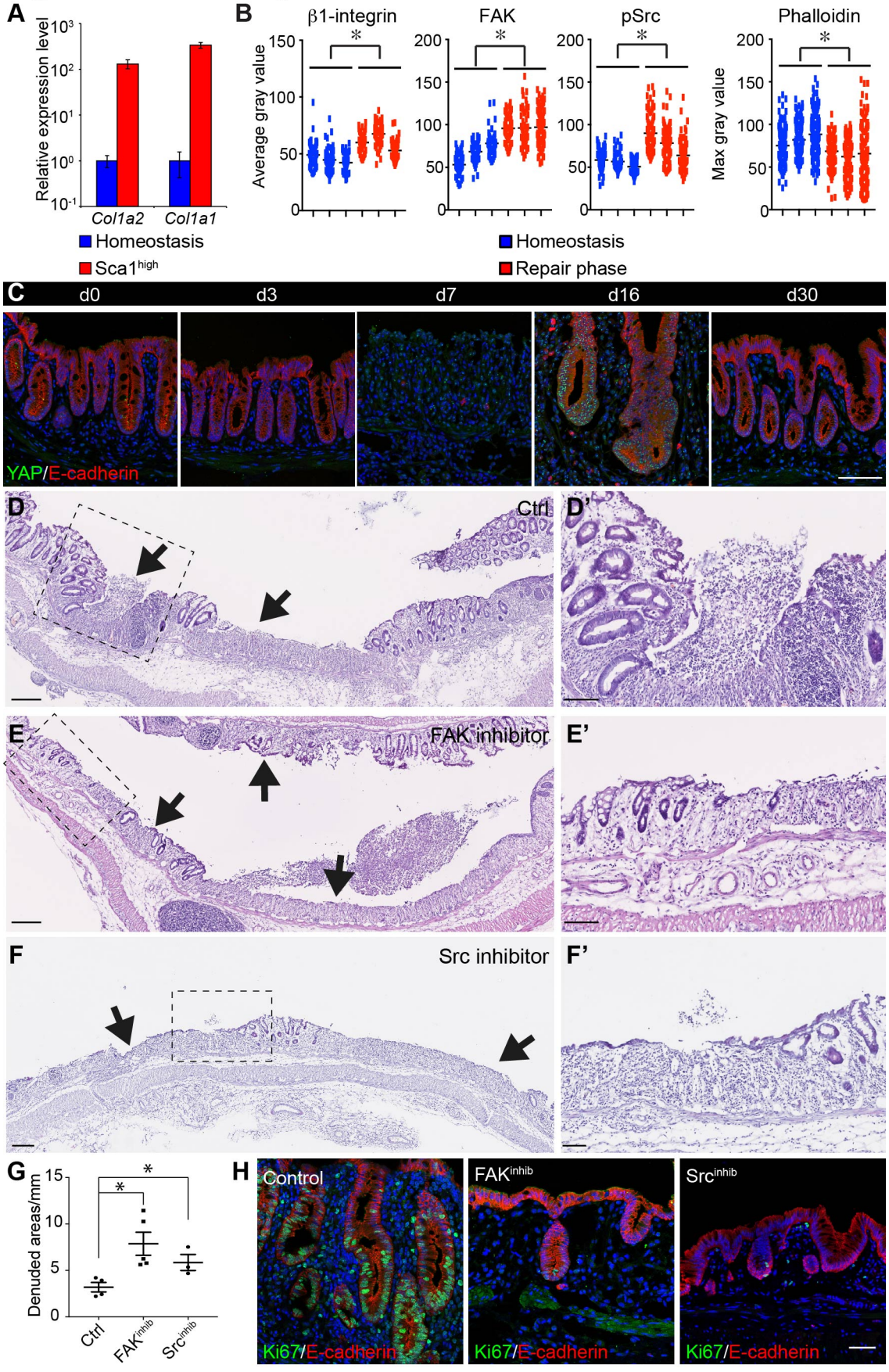

Figure S3: Characterization of the repairing epithelium

A) qPCR analysis for *Col1a2* and *Col1a1* in sorted homeostatic epithelial cells and Sca1^{high} epithelial cells. Data is presented as mean ± SEM (n=3; *Col1a2*: p=0.059; *Col1a1*: p=0.019 based on two-sided Student's t-test).

B) Quantification of confocal immunofluorescence images for β1 integrin, FAK, pSrc and Phalloidin in homeostatic and repair phase. The Y-axis represents the average gray scale value determined at the basolateral membrane for β1 integrin, FAK and pSrc, and max intensity of gray scale value determined at apical side for Phalloidin. Each dot represents single measurements. Signals were obtained for three animals per group and the average for the biological triplicates were compared (p=0.033, 0.015, 0.049 and 0.019, respectively based on two-sided Student's t-test).

C) Time course analysis for expression of YAP (green) during the course of treatment and recovery from experimental colitis. Tissue is counterstained with DAPI (blue) and E-cadherin (red). Scale bar 100μm.

D-F) Representative images from H&E stained sections of the distal part of the colon at day 12 following the administration of DSS from animals treated daily with either vehicles control (Ctrl; D) FAK inhibitor (E) or Src inhibitor (F) from day 8. Scale bar 250µm. Demarcated area is shown at higher magnification. Scale bar 100µm.

G) Length of denuded regions in the colon in the different animal groups. Each dot represent independent animals, and data is presented as the mean ± SEM (Ctrl vs FAK inhibitor p=0.016; Ctrl vs Src inhibitor p=0.037 based on two-sided Student's t-test).

H) Expression of Ki67 (green) in samples from animals treated vehicles (Ctrl), FAK or Src inhibitor. Scale bar 50µm.

Figure S4. Related to Figure 4

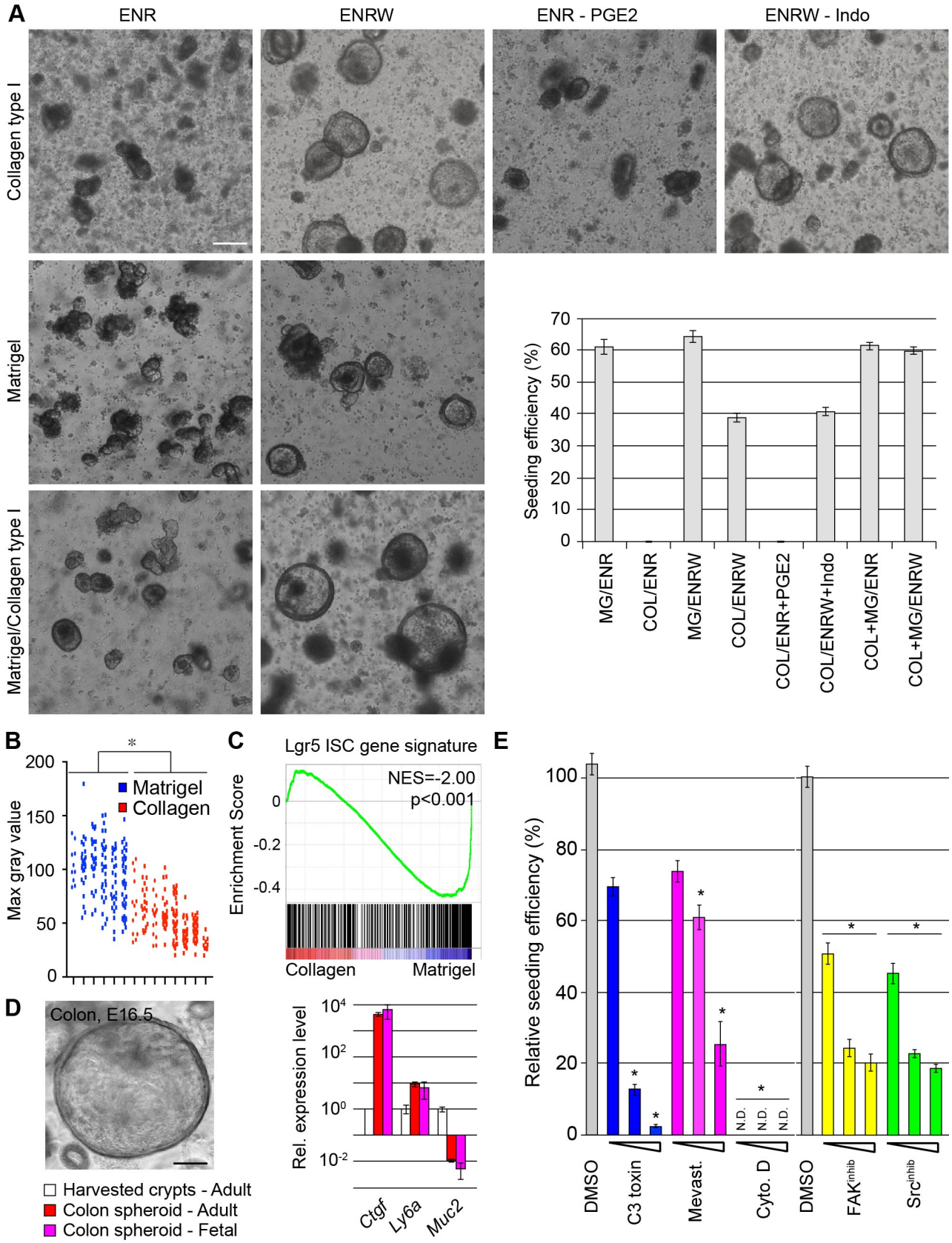

Figure S4: Recapitulating features of tissue repair *in vitro*

A) Representative images and quantification of organoid/spheroid seeding efficiency using different culture matrices and conditions. Cells were seeded in either collagen type 1, Matrigel or a 1:1 mix of collagen type 1/Matrigel cultured in either EGF/Noggin/Rspondin (ENR) or ENR supplemented with Wnt3a (W), PGE2 or Wnt3a and the Cox inhibitor Indomethacin (W – Indo). Bars represent mean ± SEM (n=3 for all conditions). Scale bar 100µm.

B) Quantification of Phalloidin localization in both Matrigel organoids and Collagen cultures. The Y-axis represents the max intensity of gray scale value determined at the apical membrane in each independent sample. Each dot represents one measurement (n=6 for Matrigel, n=8 for Collagen, $p=7.7x10^{-6}$ based on two-sided Student's t-test).

C) GSEA showing enrichment of an Lgr5 intestinal stem cell gene signature in Matrigel relative to collagen cultures.

D) Phase contrast image of fetal colonic sphere derived from E16.5 murine colon. Scale bar, 100 μm. qPCR analysis for cultured materials when compared to freshly harvested colonic crypts from adult animals. Data is presented as mean ± SEM (n=3).

E) Seeding efficiency of collagen cultures treated with C3 toxin (0.2, 1 and 3µg/mL), Mevastatin (0.3, 1 and 3µM), Cytochalasin D (0.6, 2 and 6µM), FAK-inhibitor (PF573228; 3, 5 and 10µM) and Src inhibitor (Dasatinib; 3, 5 and 10µM), when compared to samples treated with DMSO. The bars indicate the average ± SEM (n=3) ND: no growth detected (C3-toxin $p<0.0001$; Mevastatin: 1µM $p=0.02$, 10µM $p<0.0001$; Cyto D $p<0.0001$; FAK^{inhib} and Src^{inhib} $p<0.0001$ based on an ordinary one-way ANOVA test with Dunnett's multiple comparisons test with a single pooled variance).

Figure S5. Related to Figure 5

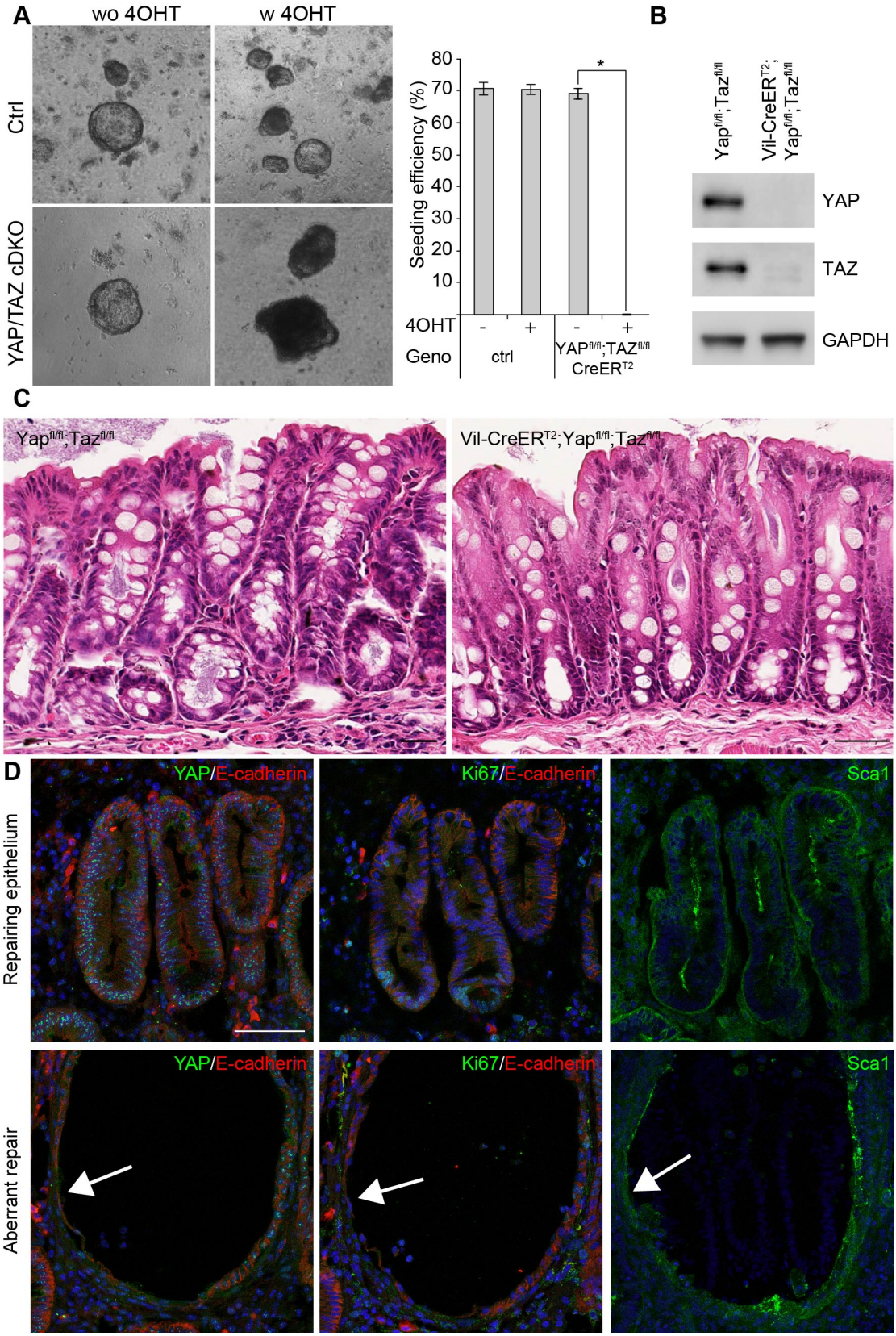

Figure S5: YAP/TAZ are required for in vitro growth and establishing the repairing epithelium expressing fetal markers

A) Seeding efficiency of control and Vil-CreER^{T2};*Yap*$^{fl/fl}$;*Taz*$^{fl/fl}$ (YAP/TAZ cDKO) spheroids cultured in collagen type 1, when exposed to 4-hydroxy tamoxifen (4OHT) following seeding. The bars indicate the average ± SEM (n=3; p=2.9x10^{-6} based on a based on two-sided Student's t-test).

B) Western Blot for YAP and TAZ from isolated small intestinal crypts 15 days after administration of tamoxifen.

c) H&E images of colon from control (*Yap*$^{fl/fl}$;*Taz*$^{fl/fl}$) and cDKO (Vil-CreER^{T2};*Yap*$^{fl/fl}$;*Taz*$^{fl/fl}$) animals 15 days after administration of tamoxifen. Scale bar 50µm.

d) Expression of Ki67, YAP and Sca1 (green) in different regions of the colon in YAP/TAZ cDKO animals at day 13 following administration of DSS reveals two distinct phenotypes either repairing epithelium or aberrant epithelial cysts. Scale bar 50µm.

Figure S6. Related to Figure 6

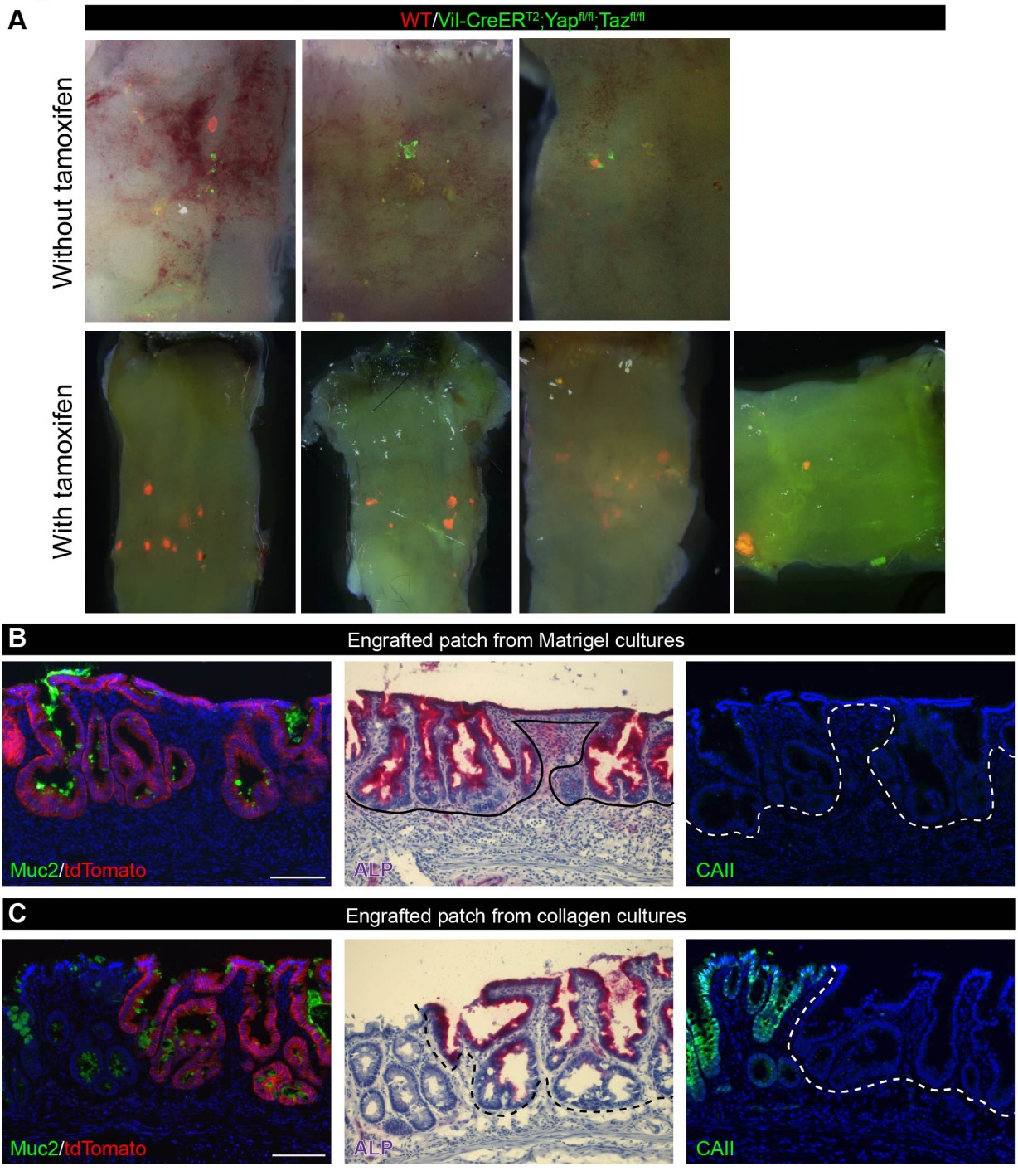

Figure S6: Tissue regeneration is recapitulated using transplantation experiments as a reversible process

A) Whole mount imaging of engrafted patches in the distal colon of animals transplanted with either wt (red) or Vil-CreER^{T2};*Yap*$^{fl/fl}$;*Taz*$^{fl/fl}$ (green) small intestinal organoids at day 8 and day 11 following initiation of DSS administration. Top panel were analyzed at day 12 (before 4-hydroxy tamoxifen treatment) and bottom panel at day 16 (3 days after 4-hydroxy tamoxifen treatment).

B-C) Detection of Mucin2 (MUC2, green, left), alkaline phosphatase (ALP, purple, middle) and carbonic anhydrase II (CAII, green, right) in transplant derived from small intestinal epithelial cells (red) cultured in Matrigel (B) or collagen type I (C). The demarcated line in serial sections indicates engrafted regions. Scale bars, 50 μm.

Supplemental Table 1. Related to Figure 1

PANTHER GO-Slim Biological Process	Total #	Observed #	Expected	Fold Enrich	P value
Lipid metabolic process	559	57	19	3.0	$2.8x10^{-10}$
Cellular amino acid metabolic process	224	30	8	3.9	$1.8x10^{-7}$
Generation of precursor metabolites and energy	227	28	8	3.6	$3.6x10^{-6}$
Fatty acid beta-oxidation	28	10	1	10.3	$1.9x10^{-5}$
Fatty acid metabolic process	195	24	7	3.6	$4.0x10^{-5}$
Respiratory electron transport chain	153	21	5	4.0	$4.1x10^{-5}$
Metabolic process	6472	282	224	1.3	$8.3x10^{-4}$
Cellular amino acid catabolic process	54	11	2	5.9	$1.0x10^{-3}$
Coenzyme metabolic process	94	14	3	4.3	$1.9x10^{-3}$
Carbohydrate metabolic process	428	34	15	2.3	$2.5x10^{-3}$
Primary metabolic process	5565	238	192	1.2	$2.8x10^{-2}$
Homeostatic process	240	21	8	2.5	$3.3x10^{-2}$

PANTHER Pathways	Total #	Observed #	Expected	Fold Enrich	P value
Pyrimidine Metabolism	10	6	0	17.4	$2.7x10^{-4}$

GO terms enriched among genes up-regulated by epithelial cell isolated from homeostatic tissue (non-DSS), when compared to $Sca1^{high}$ epithelial cells isolated during tissue repair. The table shows the number of genes in each GO category (Total #), the number of genes up-regulated in the homeostatic sample (Observed #), the relative enrichment, and the associated P-values using Bonferroni correction for multiple testing.

Supplemental Table 2. Related to Figure 1

PANTHER GO-Slim Biological Process	Total #	Observed #	Expected	Fold Enrich	P value
Cellular component morphogenesis	433	25	8	3.2	$1.4x10^{-4}$
Developmental process	1892	63	34	1.8	$5.5x10^{-4}$
Cell death	387	20	7	2.9	$9.0x10^{-3}$
Cytokine-mediated signaling pathway	122	10	2	4.5	$2.4x10^{-2}$
Locomotion	129	10	2	4.3	$3.7x10^{-2}$
Cell adhesion	369	18	7	2.7	$4.4x10^{-2}$

PANTHER Pathways	Total #	Observed #	Expected	Fold Enrich	P value
Integrin signalling pathway	191	16	3	4.6	$1.1x10^{-4}$
Inflammation mediated by chemokine and cytokine signaling pathway	262	18	5	3.8	$3.5x10^{-4}$
p53 pathway	87	8	2	5.1	$3.6x10^{-2}$
CCKR signaling map	163	11	3	3.7	$3.8x10^{-2}$

GO terms enriched among genes up-regulated by $Sca1^{high}$ epithelial cells isolated during tissue repair, when compared to epithelial cells from homeostatic conditions. The table shows the number of genes in each GO category (Total #), the number of genes up-regulated in $Sca1^{high}$ epithelial cells (Observed #), the relative enrichment, and the associated P-values using Bonferroni correction for multiple testing.